Available online at www.sciencedirect.com
ScienceDirect
Journal of the European Ceramic Society 31 (2011) 2819–2826
www.elsevier.com/locate/jeurceramsoc

High-temperature diametral compression strength of microwave-sintered mullite

P.M. Souto [a], M.A. Camerucci [b], A.G. Tomba Martinez [b,*], R.H.G.A. Kiminami [a]

[a] Departamento de Engenharia de Materiais, Universidade Federal de São Carlos, São Carlos, Brazil
[b] Laboratorio de Materiales Estructurales – División Cerámicos, INTEMA-CONICET, Mar del Plata, Argentina

Received 30 December 2010; received in revised form 14 July 2011; accepted 23 July 2011
Available online 15 August 2011

Abstract

The mechanical strength of mullite materials sintered by the conventional route or by microwave was evaluated by diametral compression at room temperature and 1400 °C. Crack patterns and fracture mechanisms were analyzed and the results were discussed in terms of the final microstructures. The conventional and microwave sintered materials showed similar densification degrees and homogeneous microstructures with small equiaxial grains. Independent of the sintering route, the fracture strength did not change as the temperature increased. However, the mechanical strength of microwave sintered mullite was always higher than the conventionally sintered materials. Moreover, in both mullite materials, microcracks produced by the effects of thermal expansion and/or elastic anisotropies during sintering and/or mechanical testing were critical defects. In the early steps, microcracks occurred in transgranular mode. However, upon approaching the critical condition, their propagation was more intergranular until they coalesced and the specimen failed, generally in a triple-cleft fracture.

Keywords: A. Microwave processing; A. Sintering; C. Mechanical properties; D. Mullite

1. Introduction

High-temperature applications of structural ceramics require optimized long-term high-temperature mechanical properties, as is well known. Maximum working temperatures are determined by the presence of intergranular glassy phases which soften at temperatures that depend on their chemical composition. Thus, the study of the mechanical properties of structural components in conditions similar to in-service ones provides key information for improving their performance.

The diametral compression test (also called the Brazilian disc test) is suitable for the mechanical evaluation of sintered ceramic materials, especially for comparative purposes. This test consists of applying a uniaxial compressive load diametrally on a disk until failure.[1,2] It has been employed mostly to evaluate green compacts and less frequently to test sintered bodies, but its use for high-temperature testing is very unusual.[3–5] The advantages of this test include simple specimen preparation and specimen geometry, rapid testing, independent surface finish data, and the absence of edge effects. However, this test may present difficulties involving changes in the load distribution due to friction in the contact zone.

Mullite is a technologically attractive material due to its excellent mechanical properties (i.e., strength and creep resistance) at high temperature, low thermal expansion ($\alpha = 4.5–5.5 \times 10^{-6}\,K^{-1}$), low thermal conductivity ($k \sim 2\,W\,m^{-1}\,K^{-1}$), low dielectric constant ($\varepsilon = 6–7$) and chemical inertness.[6–11] Therefore, mullite-based materials have been used as high-temperature structural components, infrared transparent windows and electronic packages, among other applications.[6,12] Furthermore, it has good thermal stability and requires high temperatures to achieve a high degree of densification, partly due to its low diffusion coefficient at the grain boundary.[13] Dense mullite materials have been prepared by several processing methods,[13–15] which include reaction-sintering of silica–alumina powder mixtures, solid-state sintering of fine powders prepared by several synthesis routes, etc. Microwave energy has recently emerged as a potential technology for processing ceramic materials (i.e., drying, sintering).[16–20]

* Corresponding author. Tel.: +54 223 4816600; fax: +54 223 4810046.
E-mail address: agtomba@fi.mdp.edu.ar (A.G. Tomba Martinez).

0955-2219/$ – see front matter © 2011 Elsevier Ltd. All rights reserved.
doi:10.1016/j.jeurceramsoc.2011.07.034

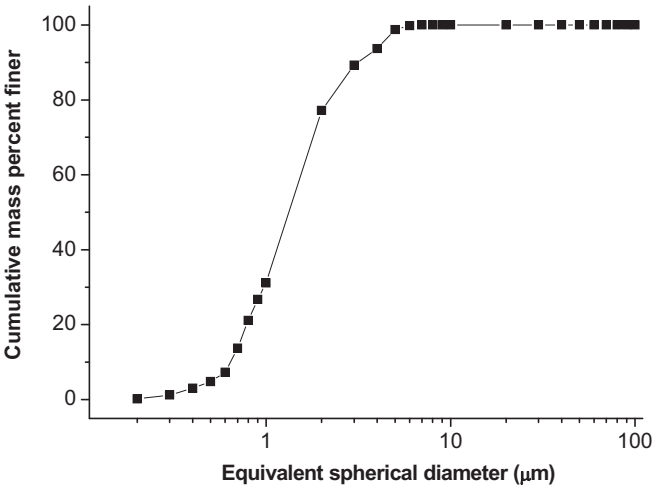

Fig. 1. Cumulative distribution of the commercial mullite powder.

In conventional thermal processing, energy is transferred to the material through convection, conduction, and radiation of heat from the surfaces of the material. In contrast, microwaves transfer energy directly into the material, where it is converted into heat by molecular interaction with the electromagnetic field. Microwave heating involves the conversion of electromagnetic energy to thermal energy rather than heat transfer. This difference in the way energy is delivered may offer many potential advantages when microwaves are used for processing materials.[16,20] Thus, because microwaves penetrate into the material, heating occurs throughout the entire volume of the material.[17] This allows thick materials to be heated rapidly and uniformly while significantly reducing their processing time and enhancing their overall quality. Some researches are using this technique to synthesize and sinter mullite.[18–24] However, data on the mechanical evaluation of mullite materials microwave-sintered at room and high temperature have not been reported in the literature yet.

The aim of this work is to evaluate the fracture strength of microwave sintered mullite disks at room and high temperatures, using the diametral compression test. For purposes of comparison, a mechanical evaluation of mullite disks sintered by the conventional route is also carried out. The results are analyzed based on the final microstructures (grain and pore sizes and morphologies, microcracks) developed by the two sintering routes, and the testing temperature.

2. Experimental

Commercially available high-purity (99.5%) mullite powder (MP40, SCIMAREC Co. Ltd., Tokyo, Japan) was used in this work.

The particle size distribution of the mullite powder was measured by a centrifugal sedimentation technique based on the principle of liquid-phase photosedimentation, using a Capa-700 particle size distribution analyzer (Horiba Instruments Ltd., Tokyo, Japan) operating at an increasing rotational speed of 460 rpm/min (Fig. 1). A mean particle size of 1.5 μm was determined. Approximately 30 wt.% of the particles showed equivalent spherical diameters of <1.0 μm and 20 wt.% had equivalent spherical diameters of >2.0 μm.

The as-received mullite powder was deagglomerated in an alcoholic medium by ball milling for 8 h. Disk-shaped samples (12 mm diameter and 3 mm thick) were prepared by unidirectional pressing at 40 MPa, followed by cold isostatic pressing (CIP) at 200 MPa. The average green density of the disks, which was determined by measuring the dimension and weight, was 58% of the theoretical density ($\delta_{th} = 3.16\ g/cm^3$).

Two sets of green samples were sintered, one set by the conventional method (CM) and the other by the microwave method (MM). Conventional sintering was performed at 1600 °C (maximum temperature of the furnace) for 2 h in an electric furnace (Lindberg/Blue M Furnace), applying a heating rate of 5 °C/min. Microwave sintering was carried out in a microwave furnace (multi-mode cavity, Cober Electronics, MS6K) at 2.45 GHz using susceptor materials as heating aids. Details of the sintering setup are given elsewhere.[21] An input power of 2.4 kW and a sintering time of 40 min at this power were used as control in the microwave sintering process (experimental drawback avoided the measurement of the sintering temperature, although it can be assured that it was higher than 1400 °C). The input power was adjusted with the aim of achieving a final volume porosity similar to that of the conventionally sintered samples. The cooling schedule was not controlled, but the entire microwave cycle (heating and cooling) took <1.7 h. The overall duration of the microwave sintering cycle was significantly shorter than the time required for the complete conventional sintering cycle (13 h).

Open porosities ($\%P_s$) of the CM and MM samples were determined by immersion in water (Archimedes method). The powdered samples were analyzed by X-ray diffraction (XRD; Siemens D-500, Cu K_α radiation, at 40 kV and 40 mA) to identify the phases present after each sintering route. The microstructural analysis was performed by scanning electron microscopy (SEM; Philips, models XL30-FEG and XL30-TMP). The surfaces to be observed by SEM were prepared according to standard ceramographic techniques (cross sections of the samples were polished and thermally etched). Grain sizes (d_g) and pore sizes (d_p) were measured using the linear-intercept technique and a stereographic correction factor of 1.56. At least 600 grains were measured in each region, using Image-Pro Plus software (Media Cybernetics).

The sintered disks were mechanically evaluated under diametral compression at room temperature (RT) and at 1400 °C, using a servohydraulic testing machine (Instron model 8501) equipped with alumina/mullite push-rods, and coupled to an electric furnace (SFL). A heating rate of 10 °C/min was employed, with a soaking time of 15 min before testing. The tests were carried out with displacement control (of the actuator), at a rate of 0.5 mm/min (duration of tests ~1–1.5 min) on a number of disks considered sufficient for statistical purposes. The diameter of the tested disks (D) was fourfold greater than the thickness (t) to ensure a plane stress state ($t/D \leq 0.25$).[5] This assumption is implicit in the theoretical treatment of diametral compression loading (Eq. (1)).[5,25,26]

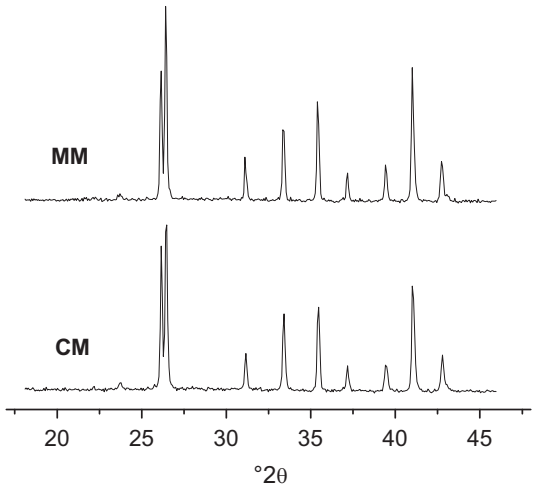

Fig. 2. XRD patterns of the sintered mullite samples.

The maximum load (P) was extracted from the experimental load vs. displacement curves to calculate the mechanical strength (σ_F), using the following relationships:

$$\sigma_F = \frac{2P}{\pi Dt} \quad (1)$$

Fracture features of tested disks were analyzed by visual inspection, while a fractographic analysis of broken specimens was performed by SEM (Jeol JSM-6460). The proportion of intergranular fracture was calculated using the SEM micrographs as the sum of intergranular mode areas in respect of the total area of the image.

3. Results and discussion

3.1. Sintered mullite materials

The open porosity values ($\%P_s$) of the CM and MM samples were very similar: $7.50 \pm 1.03\%$ for CM and $7.60 \pm 0.63\%$ for MM samples.

Fig. 2 shows XRD patterns of CM and MM. The crystalline mullite was identified in both samples (ICDD File 15-776). In addition, the absence of a baseline rising in the range of 20–30° 2θ (region of maximum diffraction peaks of silicate crystalline phases) in both X-ray patterns indicates a low content of siliceous glassy phase (<5 wt.%) in CM and MM samples.

SEM micrographs of conventional and microwave sintered mullite samples are shown in Fig. 3. Small mullite grains with a predominantly equiaxial morphology were observed in CM and MM samples. Elongated grains were scarcely observed in both types of mullite indicating a low amount of liquid phase present during sintering[11,27] which is consistent with XRD findings.

Within a similar range of sizes, the average grain size (d_g) was larger (42%) in CM (1.86 ± 1.11 μm) than in MM (1.31 ± 0.68 μm). Moreover, small asymmetric pores were dispersed throughout the volume of both samples. However, the pore sizes (d_p) of both mullite materials were similar (MM = 0.37 ± 0.21 μm and CM = 0.48 ± 0.28 μm), being in both cases fourfold lower than d_g.

3.2. Mechanical behavior

Fig. 4 shows specimens of CM and MM after mechanical testing at 1400 °C. The two materials showed the same type of fracture in the RT tests, characterized by a central fissure running along the diametral load axis (diametral fracture) together with secondary cracks parallel to the center breaking the specimens into four fragments. This type of cracks pattern, the so-called triple-cleft fracture,[1,5,28] is considered a valid mode for using Eq. (1).[1,5] The tongue and groove shape is characteristic of this type of fracture. In some cases, the specimen broke into more than four parts due to the additional failure of the internal fragments, expressing high energy stored at the time of rupture.

No deformation was observed in the contact region of the disks, where the load was applied, in any testing conditions. Moreover, the load–displacement curves were completely linear up to the sudden drop of the load when the specimens failed. This behavior was displayed at room temperature and at 1400 °C, as is observed in Fig. 5, which shows typical load–displacement curves for CM and MM specimens tested at 1400 °C. These facts evidence the absence of plasticity and the brittleness of the fracture even at 1400 °C. If glassy phase exists at the grain

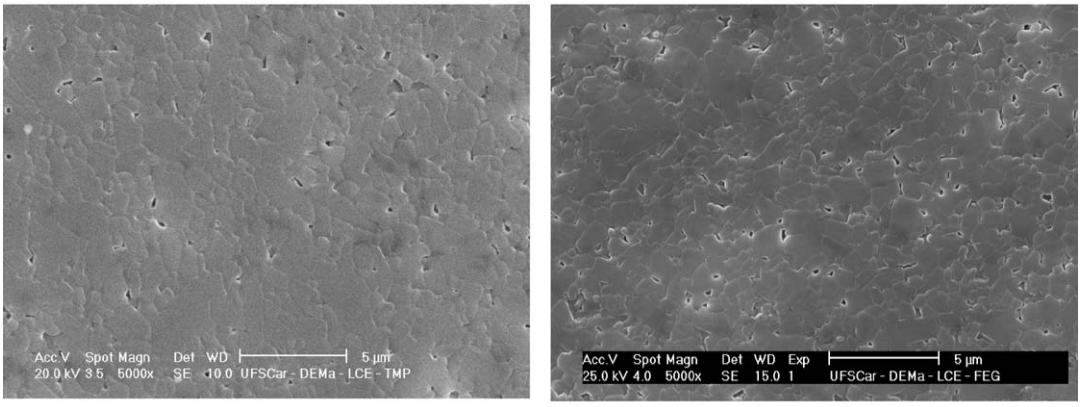

Fig. 3. SEM micrographs of samples sintered by conventional (CM) and microwave (MM) routes.

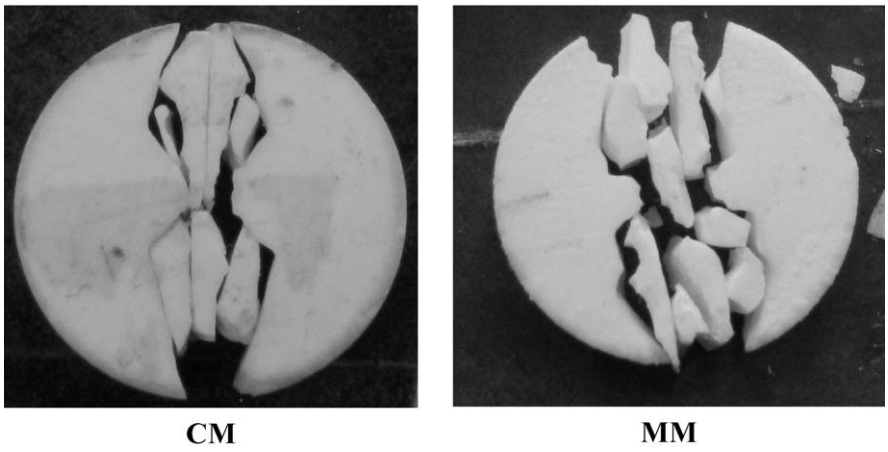

Fig. 4. Fracture patterns of CM and MM tested at 1400 °C.

boundaries, plastic deformation should occur at high temperature, as has been observed in other materials tested under similar conditions.[29,30] The brittleness of the fracture at 1400 °C would indicate that the low amount of glassy phase inferred from microstructural and mineralogical analysis is mainly confined at grain junctions[31] in both types of mullite. On the other hand, the absence of a plastic behavior validates the use of Eq. (1) to compute the fracture strength.[2,26]

Fig. 6 shows the variation in mechanical strength (σ_F) of the two mullite materials as a function of testing temperature. The mechanical strength of the conventionally sintered mullite measured at room temperature was practically the same as that determined at 1400 °C, as has been reported by other authors for similar materials.[30,31] This fact is a consequence of the materials stability due to the confinement of the low amount of glassy phase at the grain junctions. On the other hand, the mechanical strength of CM at room temperature and 1400 °C were lower than those reported in the literature for similar materials evaluated in flexure tests.[30,32] This is attributed to differences in the porosity of materials and in the type of test, since the values of mechanical strength obtained by diametral compression are always lower than those determined by flexion.[2,33] Moreover, the mechanical strength values measured for CM were lower than those obtained for MM at room temperature (considering 75.0% confidence limits) and at 1400 °C (considering 87.5% confidence limits). Similarly to CM, no significant difference between the σ_F values of MM at both testing temperatures was determined.

A discussion of the factors causing the differences between CM and MM strengths requires an analysis of the possible flaws limiting the mechanical strength of each type of material. In order to obtain a reference range for the critical flaw sizes a for each type of mullite materials, the following equation was used:

$$a = \frac{1}{\pi}\left(\frac{K_{IC}}{\sigma_F}\right)^2 \quad (2)$$

where σ_F is the stress for mode I fracture (tensile stress) and the K_{IC} is the critical stress intensity factor. Eq. (2) was applied using mechanical strength values of CM and MM corrected by porosity and by the test configuration. The correction by porosity can be carried out using Eq. (3):

$$\sigma_F = \sigma_F^0 \exp(-bp) \quad (3)$$

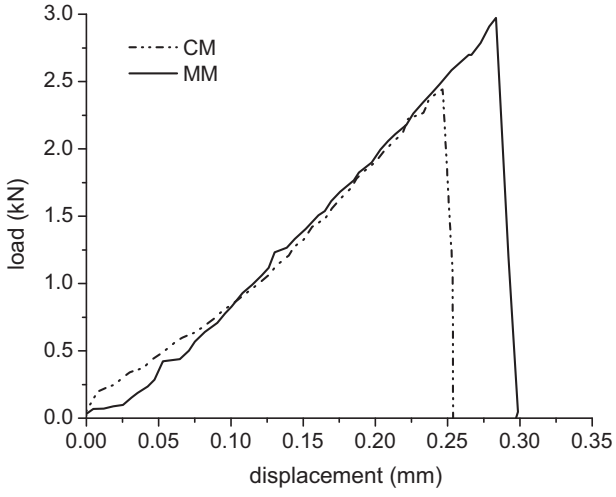

Fig. 5. Load–displacement curves of CM and MM at 1400 °C.

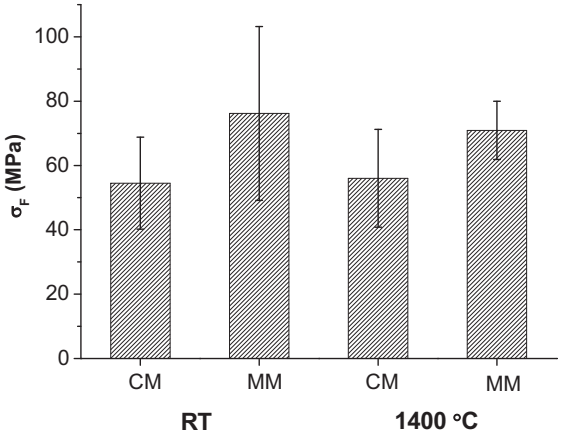

Fig. 6. Flexural strength of CM and MM as a function of testing temperature.

Table 1
Values of the corrected mechanical strength, critical flaw size and size of the limited regions with dominant transgranular mode of fracture.

T	σ_F^0 (MPa)	σ_F^{0*} (MPa)	a^0 (μm)	a^{0*} (μm)	d_t (μm)
CM RT	92 ± 24	276 ± 72	245	26	107 ± 83
1400	95 ± 26	284 ± 77	234	25	116 ± 79
MMRT	130 ± 46	389 ± 138	118	13	91 ± 63
1400	121 ± 15	361 ± 46	137	15	111 ± 76

where σ_F^0 is the mechanical strength at zero porosity, b is a parameter that depends on pore size and morphology, and p is the pore volume fraction. Table 1 shows the mean and standard deviation values of the fracture strengths of CM corrected by porosity (σ_F^0), taking a value of 7 for b.[34] The values of σ_F^0 were around three times lower than the reported strengths for similar mullite tested in flexion,[30,32] which agrees with the published differences between flexural and diametral compression strengths.[33] Then, a correction of σ_F^0 values of CM by the test configuration can be further done using a factor of 3; the corrected values (σ_F^{0*}) are also reported in Table 1. Considering 2.5 MPa $m^{1/2}$ as the value of K_{IC} for dense mullite materials taken from the literature,[14,31] the flaw sizes for CM (Table 1) were calculated based on the mean mechanical strength corrected by porosity (a^0) and also by the type of mechanical test (a^{0*}). Furthermore, based on the similar microstructure of MM and CM, the same values of b, K_{IC} and the ratio between flexural and diametral compression strengths (3) used for CM were assumed to estimate σ_F^0, σ_F^{0*}, a^0 and a^{0*} for MM materials (Table 1). The critical flaw sizes of CM and MM estimated using the above considerations were taken solely for purposes of reference for further discussion.

Among the microstructural factors (before testing) that may have been responsible for the differences between the mechanical strength of CM and MM are the pores, grain boundaries and cracks or microcracks originated during processing (although they were not observed in the SEM micrographs of the polished surfaces, Fig. 3, their presence cannot be ruled out).

The pore sizes of the conventionally sintered mullite (mean d_p: 0.48 μm) and the microwave sintered material (mean d_p: 0.37 μm) were rather smaller than the critical flaw sizes calculated as references values (a^0 and a^{0*}). Based on this finding, pores are not considered critical defects in CM and MM materials. Nevertheless, pores may interact with strength-limiting flaws and thus participate to a certain extent in the fracture of the specimens.

Secondly, grain boundaries may also act as sharp flaws due to the grooving process that occurs during the sintering heat treatment. This is one of the reasons why mechanical strength is dependent on grain size in as-fired specimens.[33] Grooving is more pronounced the higher the temperature, the longer the treatment time or the larger the grain size.[33] The microwave sintering heat treatment was significantly shorter than that of the conventional sintering which could be a reason for a more pronounced grooving in CM and therefore its lower fracture strength. Moreover, depending on grain size, the flaw leading to the fracture may involve several grains or only part of one grain. The values of d_g for both types of mullite materials were lower than the reference critical flaw sizes (Table 1). Thus, if the grain boundaries become the critical defects due to grooving, the sharp flaw thus originated would involve several grains (in the range of 14–130 grains in CM and 10–90 grains in MM).

Finally, other defects that may have governed the fracture of the materials under study were cracks or microcracks formed during the processing and/or the mechanical testing. The anisotropy of the thermal expansion coefficient (α) exhibited by mullite materials[6] induces microcraking during the material sintering (mainly in the cooling) and the mechanical tests at 1400 °C (during the heating and the soaking time). Moreover, the elastic anisotropy of mullite materials[35] may also contribute to the initiation and propagation of microcracks during the mechanical tests at both RT and 1400 °C. The fact that the coalescence of microcracks is commonly observed as the fracture mechanism in compression[33] supports the notion of microcracks as strong candidates responsible for the fracture of CM and MM materials.

Figs. 7 and 8 show SEM micrographs of fracture surfaces of CM and MM tested at RT and 1400 °C, respectively. Microwave and conventionally sintered mullites tested in both conditions showed distinct regions where different predominant fracture modes. Limited zones with different shapes and predominant transgranular fracture were visible in a matrix dominated by an intergranular mode. This change in fracture mode was reported in other works concerning the mechanical behavior of mullite flexure-tested under three- or four-point loading.[31,32,36] However, the particular distribution exhibited in the specimens evaluated in the present study has so far not been reported.

The sizes of the limited regions in which transgranular failure predominated (d_t), taken as the diameter of an equivalent sphere, were determined by analysis of the SEM micrographs (Table 1). The values of d_t for CM and MM at both testing temperatures were into the range delimited by the estimated flaw sizes of reference (a^0 and a^{0*}). Based on these findings, these limited regions would be considered microcracks acting as critical flaws in every case. The homogeneous distribution of microcracks over all the fracture surfaces (Figs. 7 and 8) was consistent with their initiation during processing or mechanical loading. The latter may occur due to the stresses distribution in the disks during the diametral compression test: the stresses are uniform through the thickness, and the tensile stresses increase toward the center of the specimen along the diameter.[26]

Taking into account the experimental error, the microcracks sizes (d_t) were similar between CM and MM at both testing temperatures, whereas the mechanical strength was lower in the former (and considering the same K_{IC} for both materials[31]). On the other hand, d_t values for MM were much more close to the respective critical flaw size a^0 (Table 1) than those of CM. This fact indicates that factors additional to the flaw size were also affecting the mechanical resistance of the materials. The flaw size distribution affects the likelihood of finding a defect of critical size and, as a consequence, the mechanical strength. The lower load bearing capacity of CM would imply a higher proportion of flaws with critical size. On the other hand, microcracks formation could be associated to the grooving of the grain boundaries (during sintering); it was considered that this process

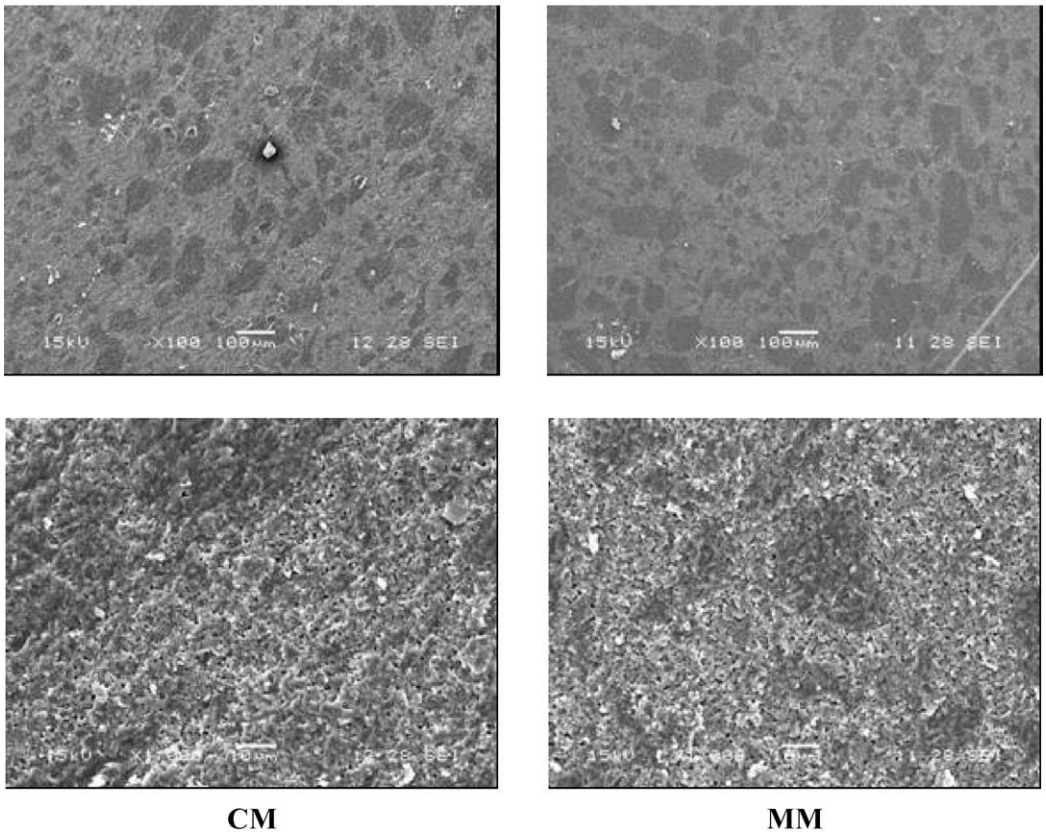

Fig. 7. SEM micrographs of fracture surfaces at room temperature.

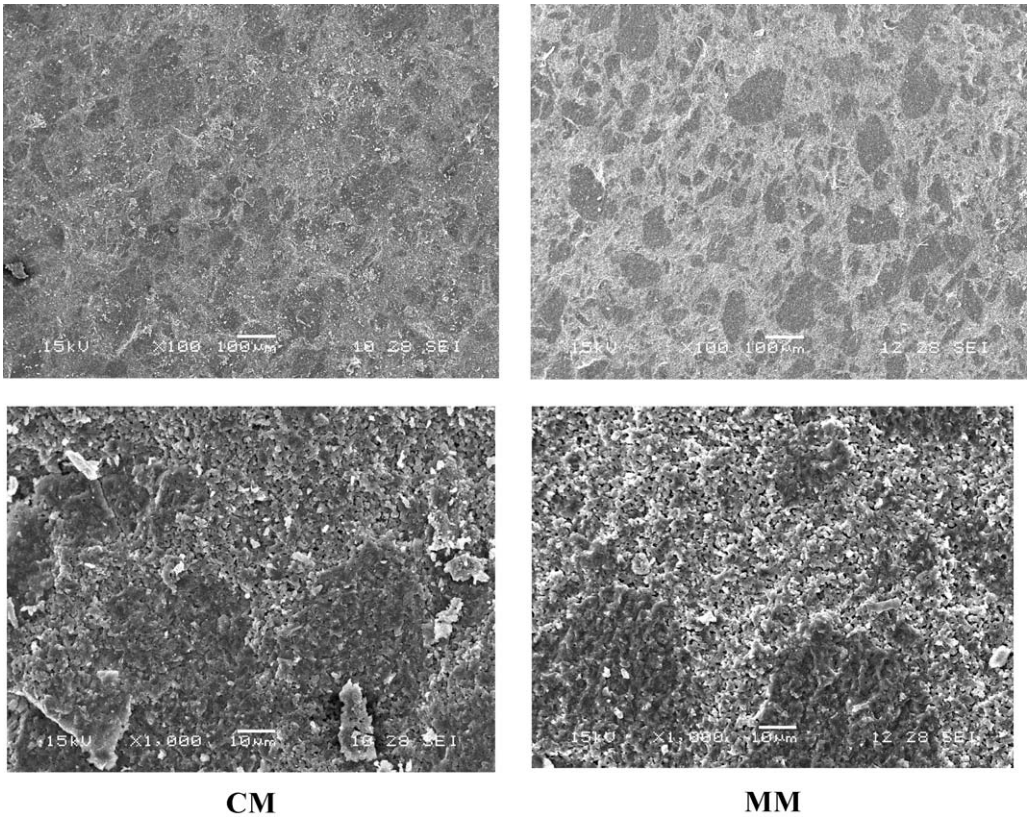

Fig. 8. SEM micrographs of fracture surfaces at 1400 °C.

was more pronounced in CM which could lead to more severe defects (i.e., with a higher capacity for stress concentration). The onset of such microcracking in association with pores was neither discarded.

Regarding the microcracking fracture mechanism (Figs. 6 and 7), microcracks propagated in a smooth, mainly transgranular mode due to the limited stress-intensity/strain-energy-density available to enable significant crack deflection or wandering.[33] This condition could be satisfied during sintering or in the first stage of mechanical testing, provided that the applied load is subcritical. Then, close to critical load conditions when the stored strain energy was high enough, the cracks grew at higher velocities and crack branching occurred, enhancing the intergranular failure. Finally, the microcracks coalesced, leading to macroscopic failure.

For the two tested mullites, the proportion of intergranular fracture mode at both mechanical testing conditions was similar (considering an experimental error of ±15%): ∼70% for CM and ∼60% for MM. This fact is consistent with the steadfast of mechanical strength values of CM and MM between RT and 1400 °C. In the presence of a glassy phase in grain boundaries, the intergranularity of failure is expected to increase at 1400 °C. The similarity of the fracture propagation between RT and 1400 °C confirm once again the presence a low content of glass phase confined to grain junctions.

The proportion of intergranular failure in CM specimens was higher than in MM (considering 75.0% confidence limits). The higher contribution of the intergranular mode to the global failure of the specimens may have been favored by grooving and by the presence of thermal expansion and elastic anisotropies.[34] The more pronounced grooving in CM specimens could account for the higher intergranularity of its fracture path.

4. Conclusions

In short, the behavior of mullite materials obtained from two different routes, conventional and microwave sintering, shows that the glassy phase (in a low amount) is confined to the grain junction and does not affect the mechanical response in the tested temperature range. The microstructure (volumetric porosity, grains morphology, content and location of glassy phase) of the mullite materials obtained by conventional (CM) or microwave (MM) sintering was similar, although the second route involved a significant reduction of the treatment duration. In spite of these microstructural similarities, the mechanical strength of MM was higher; one probable reason is the less pronounced grain boundary grooving, produced by the main effect of the sintering conditions, on the defects considered as strength limiting (microcracks).

Acknowledgements

The authors are indebted to Mr. A. Mandri and Eng. M. Pucheu (Instituto de Investigaciones en Ciencia y Tecnología de Materiales, Fac. Ingeniería, UNMdP, Argentina) for carrying out the mechanical tests. This study was supported by the CONICET (Argentina) under project (PIP 6255, 2006–2009), CAPES-CNPq (proc. 472638/2008-4) and FAPESP (proc. 2007/59564-0).

References

1. Marion RH, Johnstone JK. A parametric study of the diametral compression test for ceramics. *Am Ceram Soc Bull* 1977;**56**:998–1002.
2. Amorós JL, Cantavella V, Jarque JC, Felíu C. Green strength testing of pressed compacts: an analysis of the different methods. *J Eur Ceram Soc* 2008;**28**:701–10.
3. Tomba MAG, Reboredo M, Cavalieri AL. Characterization and mechanical behaviour of ceramics rings. *J Mater Sci* 2007;**42**(3):5036–45.
4. Sandoval ML, Pucheu MA, Talou MH, Tomba MAG, Camerucci MA. Mechanical evaluation of cordierite precursor green bodies obtained by starch thermogelling. *J Eur Ceram Soc* 2009;**29**:3307–17.
5. Darvel BW. Review uniaxial compression tests and the validity of indirect tensile strength. *J Mater Sci* 1990;**25**:757–80.
6. Schneider H, Schreuer J, Hildmann B. Structure and properties of mullite – a review. *J Eur Ceram Soc* 2008;**28**:329–44.
7. Zhang FC, Luo HH, Roberts SG. Mechanical properties and microstructure of Al_2O_3/mullite composite. *J Mater Sci* 2007;**42**:6798–802.
8. Ribeiro MJ, Labrincha JA. Properties of sintered mullite and cordierite pressed bodies manufactured using Al-rich anodising sludge. *Ceram Int* 2008;**34**:593–7.
9. Camerucci MA, Urretavizcaya G, Cavalieri AL. Evaluación Térmica Mecánica y Eléctrica de Materiales Compuestos Cordierita – Mullita. *Mater Res* 2000;**3**(4):224–30.
10. Duran C, Kemal Y. Templated grain growth of textured mullite/zirconia composites. *Mater Lett* 2005;**59**:245–9.
11. Huang T, Rahaman MN, Tai-Il M, Parthasarathay TA. Anisotropic grain growth and microstructural evolution of dense mullite above 1550 °C. *J Am Ceram Soc* 2000;**83**(1):204–10.
12. Aksay IA. Mullite for structural electronic and optical applications. *J Am Ceram Soc* 1991;**74**(10):2343–58.
13. Sacks MD, Hae-Weon Lee, Pask J. A review of powder preparation methods and densification procedures for fabricating high density mullite. *Ceram Trans* 1990;**6**:167–207.
14. Mussler BH, Shafer MW. Preparation and properties of mullite–cordierite composites. *Am Ceram Bull* 1984;**63**(5):705–14.
15. Ebadzadeh T, Lee WE. Processing-microstructure-property relations in mullite–cordierite composites. *J Eur Ceram Soc* 1998;**18**(17):837–48.
16. Menezes RR, Kiminami RHGA. Microwave sintering of alumina zirconia nanocomposites. *J Mater Process Technol* 2008;**203**:513–7.
17. Sutton W. Microwave processing of ceramic materials. *Am Ceram Soc Bull* 1989;**68**(2):376–86.
18. Ravi BG, Praveent V, Panneer Selvam M, Rao KJ. Microwave-assisted preparation and sintering of mullite – zirconia. *Mater Res Bull* 1998;**33**(10):1527–36.
19. Menezes RR, Souto PM, Fagury-Neto E, Kiminami RHGA. Microwave sintering of ceramic material. In: *The four world congress on microwave and radio frequency applications*. 2004. p. 118–32.
20. Souto PM, Menezes RR, Kiminami RHGA. Effect of Y_2O_3 additive on conventional and microwave sintering of mullite. *Ceram Int* 2011;**37**(1):241–8.
21. Souto PM, Menezes RR, Kiminami RHGA. Microwave hybrid sintering of mullite powders. *Am Ceram Soc Bull* 2007;**86**:9201–6.
22. Piluso P, Gaillard L, Lequeux N, Boch P. Mullitization and densification of ($3Al_2O_3 + 2SiO_2$) powder compacts by microwave sintering. *J Eur Ceram Soc* 1996;**16**:121–5.
23. Fang Y, Roy R, Agrawal DM. Transparent mullite ceramics from diphasic aerogels by microwave and conventional processings. *Mater Lett* 1996;**28**:11–5.
24. Souto PM. Efeito de Aditivos na Densificação e na Microestrutura da Mulita Sinterizada Convencionalmente, com Alta Taxa de Aquecimento e por Micro-ondas. Brasil: Universidade Federal de São Carlos; 2009.
25. Fahad MK. Stresses and failure in the diametral compression test. *J Mater Sci* 1996;**31**:3723–9.

26. Procopio AT, Zavaliangos A, Cunningham JC. Analysis of the diametrical compression test and the applicability to plastically deforming materials. *J Mater Sci* 2003;**38**:3629–39.
27. Metcalfe BL, Sant JH. The synthesis microstructure and physical properties of high purity mullite. *Trans Br Ceram Soc* 1975;**74**(6): 193–201.
28. Ovri JEO, Davies TJ. Diametral compression of silicon nitride. *Mater Sci Eng* 1987;**98**:109–16.
29. Sandoval ML, Talou MH, Tomba Martinez AG, Camerucci MA. Mechanical testing of cordierite porous ceramics using high temperature diametral compression. *J Mater Sci* 2010;**45**(18):5109–17.
30. Ohira H, Ismail MGMU, Yamamoto Y, Akiba Shigeyuki TS. Mechanical properties of high purity mullite at elevated temperatures. *J Eur Ceram Soc* 1996;**16**:225–9.
31. Osendi MI, Baudín C. Mechanical properties of mullite materials. *J Eur Ceram Soc* 1996;**16**:217–24.
32. Torrecillas R. Thermomechanical behaviour of mullite. *Acta Mater* 1997;**45**(3):897–906.
33. Rice RW. Mechanical properties of ceramics and composites. New York: M. Dekker, Inc.; 2000.
34. Hattiangadi A, Bandyopadhya Y. Strength degradation of nonrandom porous ceramic structures under uniaxial compressive loading. *J Am Ceram Soc* 2000;**83**(11):2730–6.
35. Ledbetter H, Kim S, Dunn M, Crudele XUZ, Kriven SW. Elastic constants of mullite containing alumina platelets. *J Eur Ceram Soc* 2001;**21**:2569–76.
36. Torrecillas R, Calderón JM, Moya JS, Reece MJ, Davies CKL, Olagon C, et al. Suitability of mullite for high temperature applications. *J Eur Ceram Soc* 1999;**19**:2519–27.